

Space group constraints on weak indices in topological insulators

Varjas, Dániel; De Juan, Fernando; Lu, Yuan Ming

DOI

[10.1103/PhysRevB.96.035115](https://doi.org/10.1103/PhysRevB.96.035115)

Publication date

2017

Document Version

Final published version

Published in

Physical Review B (Condensed Matter and Materials Physics)

Citation (APA)

Varjas, D., De Juan, F., & Lu, Y. M. (2017). Space group constraints on weak indices in topological insulators. *Physical Review B (Condensed Matter and Materials Physics)*, 96(3), Article 035115. <https://doi.org/10.1103/PhysRevB.96.035115>

Important note

To cite this publication, please use the final published version (if applicable).
Please check the document version above.

Copyright

Other than for strictly personal use, it is not permitted to download, forward or distribute the text or part of it, without the consent of the author(s) and/or copyright holder(s), unless the work is under an open content license such as Creative Commons.

Takedown policy

Please contact us and provide details if you believe this document breaches copyrights.
We will remove access to the work immediately and investigate your claim.

Space group constraints on weak indices in topological insulators

Daniel Varjas,^{1,2} Fernando de Juan,^{1,3,*} and Yuan-Ming Lu⁴

¹*Department of Physics, University of California, Berkeley, California 94720, USA*

²*QuTech and Kavli Institute of Nanoscience, Delft University of Technology, 2600 GA Delft, The Netherlands*

³*Instituto Madrileño de Estudios Avanzados en Nanociencia (IMDEA-Nanociencia), 28049 Madrid, Spain*

⁴*Department of Physics, The Ohio State University, Columbus, Ohio 43210, USA*

(Received 16 May 2017; published 10 July 2017)

Lattice translation symmetry gives rise to a large class of “weak” topological insulators (TIs), characterized by translation-protected gapless surface states and dislocation bound states. In this work we show that space group symmetries lead to constraints on the weak topological indices that define these phases. In particular, we show that screw rotation symmetry enforces the Hall conductivity in planes perpendicular to the screw axis to be quantized in multiples of the screw rank, which generally applies to interacting systems. We further show that certain 3D weak indices associated with quantum spin Hall effects (class AII) are forbidden by the Bravais lattice and by glide or even-fold screw symmetries. These results put strong constraints on weak TI candidates in the experimental and numerical search for topological materials, based on the crystal structure alone.

DOI: [10.1103/PhysRevB.96.035115](https://doi.org/10.1103/PhysRevB.96.035115)

I. INTRODUCTION

The discovery of topological insulators and superconductors is one of the most important breakthroughs of condensed-matter physics in the past decades [1–3]. The key principle underlying the existence of these novel topological phases is that the presence of a symmetry, such as time-reversal symmetry (\mathcal{T}), can lead to a quantized bulk topological invariant and robust gapless surface states. In a gapped fermion system, this invariant cannot change unless the gap closes, defining a stable quantum phase and protecting the existence of gapless boundary states. After the discovery of three-dimensional topological insulators, which are protected by \mathcal{T} , it was shown that other global symmetries in the Altland-Zirnbauer (AZ) classes [4], such as charge conjugation (\mathcal{C}) and spin rotational symmetries, can also give rise to topological phases, leading to the periodic table [5,6] of topological insulators and superconductors.

It was realized early on that additional topological phases can be obtained from invariants defined on a lower-dimensional slice of the Brillouin zone (BZ) [7]. Since this definition requires the discrete translational symmetry of the lattice, it was initially thought that these phases would not survive generic disorder and were termed “weak” topological insulators. The lower-dimensional topological invariants are therefore known as weak indices. However, further efforts then showed that weak topological phases have robust topological surface states even in the presence of impurities [8–12], and lattice dislocations therein host protected gapless modes that originate from the weak indices [13–16]. Recently it was also proposed that strong interactions can lead to novel topological orders on the surface of weak TIs [17–19]. Most of these theoretical predictions remain untested due to the difficulty of finding materials realizing these weak topological phases [20–22], though several candidates have been predicted in *ab initio* studies [23–26].

The consideration of a perfect lattice with translational symmetry immediately raises the question of whether the space group symmetries of this lattice may also have an impact on the topological properties. The addition of a space group often leads to the emergence of novel phases, generally termed topological crystalline insulators [27–44], with different properties from weak TIs. Here we address a complementary question: What are the restrictions brought by space group symmetries on possible topological phases, in particular, the weak topological phases?

In this work, we show that the nonsymmorphic elements of the space group lead to additional strong constraints for the weak indices beyond those derived from the point group. First, we show that for three-dimensional (3D) magnetic insulators in class A there is a nontrivial quantization condition on the Hall conductivity tensor in the presence of a nonsymmorphic screw symmetry. We derive this condition from band theory and then provide a general proof of its applicability to interacting systems. Second, we turn to time-reversal-invariant insulators in class AII and show how nonsymmorphic screw and glide symmetries can make the weak indices vanish in a particular direction. While enumerating every AZ symmetry class and dimensionality is beyond the scope of this paper, we present the necessary formalism to generalize our results to topological superconductors with a few examples in Appendix C.

II. CHERN NUMBER AND HALL CONDUCTIVITY (CLASS A)

A. Hall conductivity of a 3D insulator

A simple example of weak indices in a three-dimensional system is the quantized Hall conductivity of an insulator, which in proper units is given by integer-valued Chern numbers of 2D slices of the BZ. Even though these indices do not rely on translation invariance for topological protection, we also term these weak indices, as they are inherited from a lower-dimensional view on the system. Being off-diagonal elements of the conductivity tensor, these Chern numbers transform like an axial vector under point group operations.

*Present address: Rudolf Peierls Centre for Theoretical Physics, Oxford University, United Kingdom.

Here we show that a nonsymmorphic screw symmetry further imposes an important constraint on the integer-valued Hall conductivity. As we show below, this constraint holds generally for interacting systems, as long as the ground state is a nonfractionalized 3D insulator which preserves the screw symmetry. We also expect that the constraint remains valid in disordered systems that do not break the symmetry on average [8–10,16].

In a 2D system, the Hall conductance (or conductivity) σ_{xy} characterizes the transverse current response to an in-plane electric field: $j_x = \sigma_{xy} E_y$. Using the Kubo formula, one finds [45,46] that the Hall conductivity, in units of e^2/h , is given by the integral of the Berry curvature for the occupied bands over the BZ,

$$\sigma_{xy} = \frac{e^2}{h} C, \quad C = \frac{1}{2\pi} \int_{\text{BZ}} d^2\mathbf{k} \text{Tr}_{\text{occ.}} \mathcal{F}_{\mathbf{k}}, \quad (1)$$

where $\text{Tr}_{\text{occ.}}$ is the trace over occupied bands and \mathcal{F} is the Berry curvature matrix. In an insulator with a bulk gap between valence and conduction bands, the total Berry flux over the BZ is quantized to be an integer, known as the Chern number C , and hence σ_{xy} is also quantized.

In a 3D insulator the Hall conductivity becomes an antisymmetric tensor and can be cast in terms of an axial vector [46] Σ as

$$\sigma_{ij} = \frac{e^2}{2\pi h} \epsilon_{ijl} \Sigma_l, \quad \Sigma_i = \frac{\epsilon_{ijl}}{4\pi} \int_{\text{BZ}} d^3\mathbf{k} \text{Tr}_{\text{occ.}} \mathcal{F}_{\mathbf{k}}^{jl}, \quad (2)$$

where repeated indices are summed over implicitly. In band insulators this “Hall vector” is always a reciprocal lattice vector [47] and can be expressed as $\Sigma = \sum_{i=1}^3 \mathbf{G}_i C_i$, where \mathbf{G}_i are an independent set of primitive reciprocal lattice vectors, and $C_i \in \mathbb{Z}$ is the Chern-number for a cut of the BZ spanned by the other two reciprocal lattice vectors and oriented towards \mathbf{G}_i . The weak topological invariant associated with 3D insulators in symmetry class A is such a “Chern vector” $\vec{C} \in \mathbb{Z}^3$. In Appendix A we prove that the “Hall vector” transforms as an axial vector even for nonsymmorphic symmetries. This shows that lattice symmetry severely constrains its allowed values, as it has to stay invariant under every orthogonal transformation in the point group. Typically, nonzero values are allowed only with low-enough symmetry. For example, two (improper) rotations with intersecting axes are sufficient to force vanishing Hall conductance [28].

Let us impose periodic boundary condition with N_z unit cells in the direction of an arbitrary primitive lattice vector \mathbf{a}_z . Using the bulk formula, the Hall conductance of the resulting 2D system in the plane normal to \mathbf{a}_z is

$$\sigma_{xy} = \frac{1}{2} (N_z \mathbf{a}_z)_m \epsilon_{mnl} \sigma_{nl} = N_z \frac{e^2}{2\pi h} \Sigma \cdot \mathbf{a}_z = \frac{e^2}{h} N_z C_z. \quad (3)$$

Adding one extra unit cell along the \mathbf{a}_z direction will increase the normal Hall conductance by exactly the Chern number C_z in units of e^2/h . In an anisotropic limit the 3D insulator can be viewed as a stack of 2D layers with a quantized Hall conductance $\sigma_{xy}^L = \frac{e^2}{h} C_z$ each. Therefore, the Hall conductivity tensor (2) is nothing but the Hall conductance per unit cell layer, σ_{xy}^L , which can be defined as the difference between the Hall conductances of the N_z and the $N_z + 1$ layers. As will

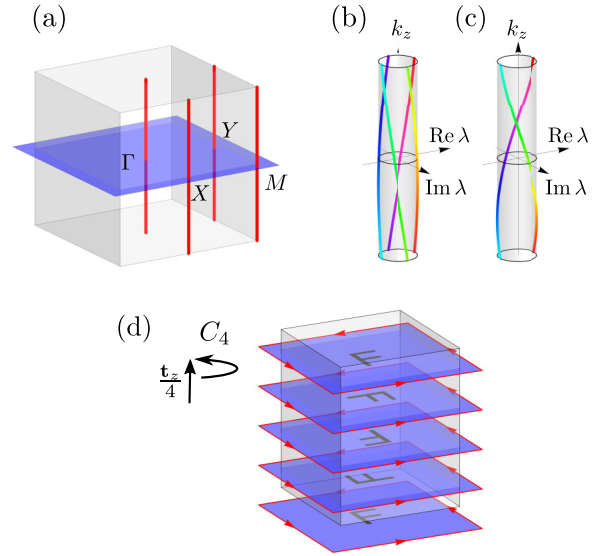


FIG. 1. (a) Brillouin zone of an insulator with fourfold screw symmetry. The perpendicular plane through the BZ center (blue) contains four high-symmetry points; we use the formula relating the Chern number to rotation eigenvalues at these points. There are four invariant lines in the direction of the screw axis (red). (b),(c) The screw eigenvalues λ evolve into each other along the fourfold (twofold) screw-invariant lines through Γ and M (X and Y). The values trace spirals as the function of k_z , the complex phase also illustrated by color code. (d) Intuitive real-space picture of the screw operation and a symmetric insulator as a stack of integer Chern insulator layers related by the screw. The unit cell contains four layers, so the Hall conductance per transverse unit cell is a multiple of 4.

become clear later, this difference σ_{xy}^L does not depend on N_z as long as N_z is much larger than the correlation length, so we adopt this definition for our interacting proof.

In the following we show that, with a nonsymmorphic n -fold screw symmetry, the Hall conductance per unit cell layer along the screw-axis direction cannot be an arbitrary integer (in units of e^2/h) for a gapped 3D insulator without fractionalization. Instead, it must be a multiple of n , as enforced by the screw symmetry.

B. Screw symmetry enforced constraints

Below we will show the Chern number for a cut perpendicular to an n -fold screw axis is quantized to a multiple of n . Consider an essential n -fold screw in the z direction; by essential screw we mean a space group (SG) operation that leaves no point in space invariant up to lattice translations [48]. We assume that the translation part is $1/n$ of the primitive lattice vector parallel to the n -fold rotational axis [49], $g = \{C_n | \mathbf{a}_z/n\}$. We invoke results [28,40,50] that allow calculation of the Chern number in the presence of n -fold rotational symmetry in 2D as a product of rotation eigenvalues of occupied bands at high-symmetry points of the BZ. For example, with C_4 symmetry [Fig. 1(a)],

$$\exp\left(2\pi i \frac{C}{4}\right) = \prod_{m \in \text{occ.}} \xi_m^\Gamma(C_4) \xi_m^M(C_4) \xi_m^X(C_4^{-2}), \quad (4)$$

where $\xi_m^{\mathbf{k}}(O)$ is the rotation eigenvalue of O in band m at momentum \mathbf{k} . Similar formulas can be derived for rotations C_2 , C_3 , and C_6 .

When restricted to the 2D cut of the BZ through Γ , a screw acts the same way as a symmorphic C_n rotation, so the formula can be applied. Now consider the high-symmetry lines in the BZ, parallel to the screw axis [vertical lines in Fig. 1(a)]. As the n th power of the screw $g^n = (-1)^F \{1|\mathbf{a}_z\}$ is a pure translation up to fermion parity, the eigenvalues of screw g take values of $\lambda = \exp(i\mathbf{k} \cdot \mathbf{a}_z/n + 2\pi im/n + \pi i F/n)$ for $m \in \mathbb{Z}_n$ [Figs. 1(b) and 1(c)]. When restricted to the perpendicular plane with $\mathbf{k} \cdot \mathbf{a}_z = 0$, the eigenvalues are simply the n th roots of fermion parity $(-1)^F$. Increasing k_z by 2π changes the eigenvalue of g by a factor of $e^{2\pi i/n}$, leading to an n -multiplet of occupied bands at each screw-invariant momentum. This shows that the product of screw eigenvalues at high-symmetry points is always 1 for every gapped band structure. This immediately proves that

$$\frac{\sigma_{xy}^L}{e^2/h} = C_z \equiv 0 \pmod{n}. \quad (5)$$

In the following we show that this result is not a peculiarity of band theory for free electrons, but holds for any gapped unique ground state preserving n -fold screw symmetry, even in the presence of interactions. The proof is based on the following cut-and-glue procedure. We start with a slab containing $N_z + m/n$ unit cells along the z direction, which is parallel to the screw axis. While this number of unit cells is not integer, screw symmetry allows us to identify the top and bottom surfaces using a boundary condition twisted by a C_n rotation [51], which results in a screw symmetric bulk without boundaries [Fig. 2(a)]. To take the thermodynamic limit, we assume the size of the system is much larger than the correlation length of the gapped bulk. To define the Hall conductance σ_{xy} in this geometry, we invoke the Streda

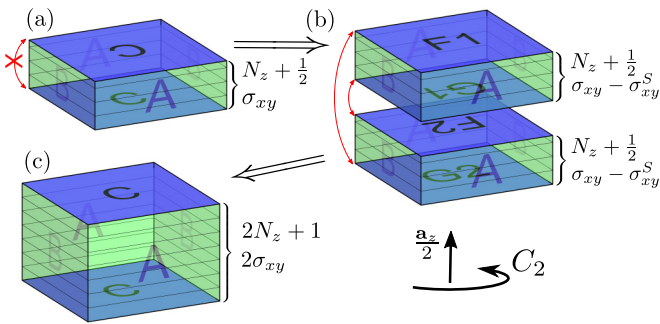


FIG. 2. The process used in the general proof for the Hall conductance constraint (5), illustrated in the case of a twofold screw. (a) A thick slab with half-integer thickness and twisted periodic boundary condition in the z direction. As we open the boundary condition in the z direction, the Hall conductance may change by a surface contribution $-\sigma_{xy}^S$. (b) We combine two slabs; the screw axis makes it possible to arrange these such that the interfaces are guaranteed to be identical: A top surface (F) meets a bottom surface (G) with the same orientation. Gluing the two interfaces together each contributes $+\sigma_{xy}^S$. (c) The resulting system has periodic boundary conditions in all three directions with odd thickness, while the Hall conductance is an even multiple of the conductance quantum.

formula [52], whereby the Hall conductance is given by the charge bound to a localized 2π flux threaded through the system. Unless the charge captured is an integer, the system is fractionalized and has degenerate ground states, contradicting our initial assumption.

Next we cut the system open in the z direction. During this process we change the Hall conductance by a surface contribution of $-\sigma_{xy}^S$. σ_{xy}^S can depend on the thickness, but should saturate to a thickness-independent constant, as long as N_z is much larger than the correlation length of the gapped bulk. We then take n copies of this open system and arrange them along the z direction related by C_n rotations such that all the interfaces are symmetry related [Fig. 2(b)]. Gluing the surfaces together by restoring the screw symmetric bulk Hamiltonian changes the Hall conductance by σ_{xy}^S at each interface, as the separation between them is much larger than the bulk correlation length. The resulting system [Fig. 2(c)] has periodic boundary conditions in all three directions with a thickness of $nN + m$ unit cells and Hall conductance of $n(\sigma_{xy} - \sigma_{xy}^S) + n\sigma_{xy}^S = n\sigma_{xy}$. Thus, we proved that a sample with arbitrary integer thickness has a Hall conductance which is a multiple of n times the conductance quantum.

III. WEAK TI INDICES (CLASS AII)

A. Constraints from Bravais lattice

We now consider time-reversal symmetric insulators in class AII. To calculate the weak \mathbb{Z}_2 invariants, we evaluate [7]

$$v_i = \frac{1}{2\pi} \text{Tr}_{\text{occ.}} \left(\int_{\frac{1}{2}T^2} \mathcal{F}_{\mathbf{k}} d^2\mathbf{k} - \oint_{\partial \frac{1}{2}T^2} \mathcal{A}_{\mathbf{k}} \cdot d\mathbf{k} \right) \pmod{2}, \quad (6)$$

where \mathcal{A} and \mathcal{F} are the Berry curvature and connection, respectively, and the integral is over the interior and boundary of half of the time-reversal-invariant 2D cut of the BZ spanned by the two reciprocal lattice vectors other than \mathbf{G}_i and offset from the Γ point by $\mathbf{G}_i/2$. Expanding the momentum vector in a primitive reciprocal lattice vector basis as $\mathbf{k} = \frac{1}{2\pi} \sum_{j=1}^3 k_j \mathbf{G}_j$, these planes are defined by $k_i = \pi$ and form a face of the parallelepipedal reciprocal unit cell centered around Γ . The weak indices define a \mathbf{k} -space vector, pointing to one of the eight TR-invariant momenta (TRIM):

$$\mathbf{G}^v = \frac{1}{2} v_i \mathbf{G}_i. \quad (7)$$

This vector is independent of the choice of the unit cell [38] and transforms under space group operations as \mathbf{k} -space vectors (see Appendix A). One can enumerate the allowed values of \mathbf{G}^v by inspecting tables for Wyckoff positions of the reciprocal space groups: \mathbf{G}^v can only take values at points with half-integer Miller indices that are invariant under the point group up to reciprocal lattice vectors. For example, a face-centered cubic lattice (as realized in the diamond structure [54]) cannot support nontrivial weak indices without breaking point group symmetries, simply because no TRIM is left invariant under the point group except Γ . These types of constraints, enforced only by the type of Bravais lattice [55], are listed in Table I.

These results can also be rationalized from the band inversion point of view. To get a nontrivial weak index, we

TABLE I. Constraints on possible weak indices based on the Bravais lattice in time-reversal-invariant insulators. The allowed values of \mathbf{G}^v are labeled according to the convention for high-symmetry momenta in International Tables for Crystallography (ITA) [53]; “all” means all the eight possible values are allowed.

Crystal system	Centering	Allowed values of \mathbf{G}^v
Triclinic	P	All
Monoclinic	P	All
	C	Γ, Y, A, M
Orthorhombic	P	All
	C	Γ, Y, T, Z
	I	Γ, X
	F	Γ, Y, T, Z
Tetragonal	P	Γ, Z, M, A
	I	Γ, M
Trigonal	P	Γ, A
	I	Γ, T
Hexagonal	P	Γ, A
	F	Γ, R
Cubic	I	Γ, H
	F	Γ

need an odd number of band inversions among the four TRIMs located on a plane offset by $\mathbf{G}_i/2$ (defined as above), and only the band inversions at the four TRIMs here contribute to the weak index ν_i . However, point group symmetry relates some of these TRIMs, and band inversion has to occur on all symmetry related points simultaneously. For example, in the bcc reciprocal crystal TRIMs are symmetry equivalent in such a fashion that there is an even number of related points in any of these offset planes, explaining the lack of nontrivial weak TIs. On the other hand, a strong TI is possible with any SG, as the Γ point is always of maximal symmetry and it is possible to have a band inversion only at Γ (see Appendix D).

B. Constraints from nonsymmorphic symmetries

The presence of nonsymmorphic symmetries leads to further constraints on the weak indices. We now show that in the presence of an essential twofold screw in the z direction, the weak index must be trivial in this direction. First we note that a twofold screw $\{C_2|\mathbf{a}_z/2\}$ with \mathbf{a}_z a primitive lattice vector, squares to $\{-\mathbb{1}|\mathbf{a}_z\}$, represented at $k_z = \pi$ as $+\mathbb{1}$, which commutes with \mathcal{T} . For now we assume the other two primitive lattice vectors are perpendicular to \mathbf{a}_z and in the $k_z = \pi$ plane the screw acts like a proper inversion in a 2D system. We use the known result to evaluate the weak index by counting inversion eigenvalues [27]; it is given by the total number of occupied Kramers pairs with -1 inversion eigenvalue at the four TRIMs modulo 2. In this plane Kramers partners have the same screw eigenvalues, as required.

However, this situation in a 3D system with screw is different from a 2D system with a symmorphic inversion symmetry in that the screw requires an equal number of both screw eigen-

values below the gap, as shown earlier. Specifically at $k_z = \pi$ at each high-symmetry point the number of occupied $+1$ and -1 eigenvalues must be equal, and as the number of occupied bands is constant, the total number of occupied -1 bands is a multiple of 4, leading to a trivial \mathbb{Z}_2 index in this plane.

In general, a weak vector in the presence of an essential screw $\{C_2|\mathbf{a}_z/2\}$ is allowed only if

$$\mathbf{G}^v \cdot \mathbf{a}_z \equiv 0 \pmod{2\pi}. \quad (8)$$

We analogously argue [31,32] that an essential glide forbids nontrivial weak index in the direction parallel to the translational part of the glide. Again, a diagonal glide is never essential, and the constraint follows from Bravais-lattice considerations. In general, an essential glide with in-plane translation $\mathbf{a}_z/2$ allows a weak vector only if $\mathbf{G}^v \cdot \mathbf{a}_z \equiv 0 \pmod{2\pi}$, consistent with the analysis of the “hourglass” surface states [37,40].

IV. CONCLUSION

In summary, we derived a set of constraints on weak topological indices in 3D insulators from nonsymmorphic and symmorphic space group symmetries. We showed that in the presence of n -fold screw rotation, Hall conductivity must be quantized as a multiple of n for any 3D nonfractionalized insulator preserving screw symmetry. This condition is generally proved for interacting systems. We also showed certain 3D weak indices for TIs (class AII) are forbidden by the Bravais lattice and glide or even-fold screw symmetries. These Bravais-lattice constraints can also be applied to weak indices in topological superconductors; see Appendix C. These results put strong constraints on the candidates for weak topological phases in the ongoing experimental and numerical efforts to find physical realizations of these novel topological phases.

ACKNOWLEDGMENTS

The authors are grateful to T. Morimoto and H. C. Po for helpful conversations. This work is supported by NSF Grant No. DMR-1206515 (D.V. and F.d.J.), the Netherlands Organization for Scientific Research (NWO), the Foundation for Fundamental Research on Matter (FOM) (D.V.), the European Research Council Advanced Grant (Contract No. 290846) (F.d.J.), and startup fund at Ohio State University (Y.-M.L.).

APPENDIX A: PROOF FOR TRANSFORMATION PROPERTIES OF WEAK INDICES

First we review the representations of space group operations in \mathbf{k} space [40,41]. We use the convention (Appendix B) with Bloch basis functions $|\chi_{\mathbf{k}}^{\mathbf{x}l}\rangle = \sum_{\mathbf{R}} e^{i\mathbf{k}(\mathbf{R}+\mathbf{x})} |\phi_{\mathbf{R}+\mathbf{x}}^l\rangle$, where we split the orbital index $a = (\mathbf{x}, l)$, \mathbf{x} labels the sites of the unit cell by their real-space position and l is an on-site orbital index accounting for spin, orbital angular momentum, etc. (the values l can take may depend on \mathbf{x}). A useful property of this basis is that it is periodic in the real-space coordinate; i.e., $|\chi_{\mathbf{k}}^{(\mathbf{x}+\mathbf{R})l}\rangle = |\chi_{\mathbf{k}}^{\mathbf{x}l}\rangle$ for any lattice vector \mathbf{R} . We emphasize that our treatment is not specific to tight-binding models; the same can be told in the continuum, where \mathbf{x} is the continuous

index for position in the unit cell and l stands for the spin only. To go to the tight-binding approximation, we restrict the Hilbert space to a finite set of orbitals per unit cell; the only assumption we make is that orbitals centered on different sites span orthogonal subspaces.

Consider a general space group operation $g = \{O|\mathbf{t}\}$ acting on one of the basis states,

$$g|\phi_{\mathbf{R}+\mathbf{x}}^l\rangle = U_{\mathbf{x}}^{ll'}|\phi_{g(\mathbf{R}+\mathbf{x})}^{l'}\rangle = U_{\mathbf{x}}^{ll'}|\phi_{O(\mathbf{R}+\mathbf{x})+\mathbf{t}}^{l'}\rangle, \quad (\text{A1})$$

where U is the site and g -dependent unitary representation on the local orbitals, a double representation if the model is spinful. Applying this to the Bloch basis functions, with simple algebra we find

$$g|\chi_{\mathbf{k}}^{xl}\rangle = e^{-i(g\mathbf{k})\mathbf{t}} U_{\mathbf{x}}^{ll'}|\chi_{g\mathbf{k}}^{x'l'}\rangle, \quad (\text{A2})$$

with $g\mathbf{k} = O\mathbf{k}$ and $g\mathbf{x} = O\mathbf{x} + \mathbf{t}$ that is understood as a permutation of sites at the same Wyckoff position. Grouping indices back together, this can be written as $g|\chi_{\mathbf{k}}^a\rangle = e^{-i(g\mathbf{k})\mathbf{t}} U^{ba}|\chi_{g\mathbf{k}}^b\rangle$.

The key observation is that in this basis the \mathbf{k} dependence decouples as a single factor proportional to the identity. Consider the transformation of a Bloch eigenstate in the n th band, $|n_{\mathbf{k}}\rangle = n_{\mathbf{k}}^a|\chi_{\mathbf{k}}^a\rangle$. The symmetry transformation results in a state at $g\mathbf{k}$; the coefficients transform as $(gn)_{g\mathbf{k}}^a = e^{-i(g\mathbf{k})\mathbf{t}} U^{ab} n_{\mathbf{k}}^b$ or in a compact notation $g(n_{\mathbf{k}}) = (gn)_{g\mathbf{k}} = e^{-i(g\mathbf{k})\mathbf{t}} U n_{\mathbf{k}}$. As g is a symmetry operation, the transformed state is again an eigenstate of the Bloch Hamiltonian with the same energy, but at $g\mathbf{k}$. As a consequence, the transformation of occupied band projector operator $\mathcal{P}_{\mathbf{k}} = \sum_{n \in \text{occ.}} n_{\mathbf{k}} n_{\mathbf{k}}^\dagger$ reads

$$(g\mathcal{P})_{g\mathbf{k}} = \sum_{n \in \text{occ.}} (gn)_{g\mathbf{k}} (gn)_{g\mathbf{k}}^\dagger = U \mathcal{P}_{\mathbf{k}} U^\dagger. \quad (\text{A3})$$

So if g is a symmetry, such that $(g\mathcal{P})_{\mathbf{k}} = \mathcal{P}_{\mathbf{k}}$, any gauge-invariant quantity that can be expressed through $\mathcal{P}_{\mathbf{k}}$ is invariant if the \mathbf{k} -space coordinates are transformed accordingly. Examples include [41] the Berry curvature $\mathcal{F} = i\mathcal{P}d\mathcal{P} \wedge d\mathcal{P}$ and closed loop integrals of the Berry connection \mathcal{A} (see below).

The ‘‘Hall vector’’ as defined in Eq. (2) may be cast in a coordinate free form, as

$$\Sigma = \frac{1}{2\pi} \int \text{Tr } \mathcal{F} \wedge d\mathbf{k}. \quad (\text{A4})$$

To see that it is equal to $\sum_{i=1}^3 \mathbf{G}_i \mathcal{C}_i$, it is sufficient to check that $\mathbf{a}_i \cdot \Sigma$ is the same in the two cases for all lattice vectors. Simple substitution shows that this vector transforms as an axial vector under all SG operations [i.e., even under inversion, $\Sigma \rightarrow (\det O)O\Sigma$], as stated in the main text.

For completeness we derive the transformation properties of \mathcal{A} and \mathcal{F} under the basis change corresponding to switching between conventions and show that invariants calculated in either convention give the same result. (For details about the two conventions, see Appendix B.) We feel this is necessary because, while the Berry connection for the Bloch basis $|\tilde{\chi}_{\mathbf{k}}^a\rangle$ vanishes and one can safely use the coefficients, for the basis $|\chi_{\mathbf{k}}^a\rangle$ it is nonzero, $\mathcal{A}_{\chi}^{ab} = i\langle \chi_{\mathbf{k}}^a | d | \chi_{\mathbf{k}}^b \rangle = i\delta^{ab} e^{i\mathbf{k}\mathbf{t}_a} \mathbf{t}_a d\mathbf{k}$. This

means that one may worry that the formulas in terms of the components in this basis may be missing some terms coming from the derivatives of the basis vectors.

For generality, we consider a transformation $U_{\mathbf{k}}$ acting on the coefficients, it may either be a basis transformation or a physical one, and let $n_{\mathbf{k}}' = U_{\mathbf{k}} n_{\mathbf{k}}$. We find

$$\text{Tr}_{\text{occ.}} \mathcal{A}' = \sum_n i n^{\dagger} d n' = \text{Tr}_{\text{occ.}} \mathcal{A} + i \text{Tr}(\mathcal{P} U^\dagger d U), \quad (\text{A5})$$

$$\text{Tr}_{\text{occ.}} \mathcal{F}' = \text{Tr}_{\text{occ.}} d \mathcal{A}' = \text{Tr}_{\text{occ.}} \mathcal{F} + i d \text{Tr}(\mathcal{P} U^\dagger d U), \quad (\text{A6})$$

where $\text{Tr}_{\text{occ.}}(\cdot) = \sum_n (\cdot)^{nn}$ is the trace over occupied bands, while $\text{Tr}(\cdot) = \sum_a (\cdot)^{aa}$ is the trace over the entire Hilbert-space of the unit cell. We see that as long as $\mathcal{P} U^\dagger d U$ is unit cell periodic, which is the case for the basis transformation, $U_{\mathbf{k}}^{ab} = W_{\mathbf{k}}^{ab} = \delta^{ab} e^{i\mathbf{k}\mathbf{r}_a}$ if $\mathcal{P} = \tilde{\mathcal{P}}$ (BZ periodic convention). The change in $\text{Tr}_{\text{occ.}} \int_S \mathcal{F}$ is fully compensated by the change in $\text{Tr}_{\text{occ.}} \int_{\partial S} \mathcal{A}$ in the formula for the \mathbb{Z}_2 invariants and vanishes for Chern numbers.

We note that the expression for $\text{Tr}_{\text{occ.}} \oint \mathcal{A}$ along a noncontractible loop in terms of the projector is modified in the $|\chi\rangle$ basis,

$$\text{Tr}_{\text{occ.}} \oint \mathcal{A} = i \ln \det_+ \left(W_{-\mathbf{G}} \prod_{\mathbf{k}=\mathbf{k}_0}^{\mathbf{k}_0-\mathbf{G}} \mathcal{P}_{\mathbf{k}} \right), \quad (\text{A7})$$

where \det_+ is the pseudodeterminant of the matrix, which is defined as the product of all nonzero eigenvalues. This is equivalent to calculating the determinant of the restriction to the local occupied space at \mathbf{k}_0 ; i.e., we evaluate $-i \ln \det_+$ as the sum of the complex phases of the nonzero eigenvalues. The reason $W_{\mathbf{G}}$ appears is the mismatch of the basis at \mathbf{k}_0 and $\mathbf{k}_0 + \mathbf{G}$.

APPENDIX B: CONVENTIONS FOR BLOCH FUNCTIONS

There are two widely used conventions to define the Bloch basis functions. When appropriate we use the convention where we define Bloch basis functions $|\tilde{\chi}_{\mathbf{k}}^a\rangle$ in terms of the orbitals of the unit cell $|\tilde{\chi}_{\mathbf{k}}^a\rangle = \sum_{\mathbf{R}} e^{i\mathbf{k}\mathbf{R}} |\phi_{\mathbf{R}}^a\rangle$, where \mathbf{R} is the unit cell coordinate and a the orbital index. Note the absence of phase factors corresponding to the position of the orbitals within the unit cell, so the basis functions are strictly periodic in the BZ. While in this convention the information about the position of the orbitals is lost; thus, the polarizations computed via Berry vector potential integrals do not equal the true Wannier center positions. The Bloch Hamiltonian is BZ periodic, making some derivations more transparent.

In the other convention we define $|\chi_{\mathbf{k}}^a\rangle = \sum_{\mathbf{R}} e^{i\mathbf{k}(\mathbf{R}+\mathbf{r}_a)} |\phi_{\mathbf{R}}^a\rangle$, where \mathbf{r}_a is the position of the a th orbital in the unit cell. The two conventions are related by the operator $W_{\mathbf{k}}$ with $W_{\mathbf{k}}^{ab} = \delta^{ab} e^{-i\mathbf{k}\mathbf{r}_a}$ such that $|\chi_{\mathbf{k}}^a\rangle = (W_{\mathbf{k}}^{-1})^{ab} |\tilde{\chi}_{\mathbf{k}}^b\rangle$ so the coefficients of Bloch wave functions transform as $n_{\mathbf{k}}^a = W_{\mathbf{k}}^{ab} \tilde{n}_{\mathbf{k}}^b$. Consequently, operators expanded in this basis (including the Bloch Hamiltonian) satisfy $O_{\mathbf{k}+\mathbf{G}} = W_{\mathbf{G}} O_{\mathbf{k}} W_{\mathbf{G}}^{-1}$, where \mathbf{G} is a primitive reciprocal lattice vector. $W_{\mathbf{G}} : \mathcal{H}_{\mathbf{k}} \rightarrow \mathcal{H}_{\mathbf{k}+\mathbf{G}}$ is acting between the Hilbert spaces of the coefficients of the wave functions in this basis. This convention, using the

coefficients only (e.g., $\mathcal{A}^{nm} = in^\dagger dm$), is usually assumed in formulas for electromagnetic response, as the naive Peierls substitution $\mathbf{k} \rightarrow \mathbf{k} + \mathbf{A}$ only gives the correct phase factor for hopping in this case. The two conventions give equivalent results for quantized topological indices in most symmorphic cases, provided there is a continuous, symmetry-preserving deformation of the lattice, such that all the orbitals are brought to the same point in the unit cell. In nonsymmorphic lattices, however, this is never possible, as the shortest orbit of a point in the unit cell under the symmetry group modulo lattice vectors is longer than one; there is no crystal with one site per unit cell obeying a nonsymmorphic symmetry. For example, with an n -fold screw translating in the z direction one needs at least n lattice sites that can be arranged such that the positions are $\mathbf{r}_a = \mathbf{a}_z a/n$ for $a = 1, \dots, n$, so $W_{\mathbf{G}_z}^{ab} = \delta^{ab} e^{2\pi i a/n}$ and $W_{\mathbf{G}} = \mathbb{1}$ for perpendicular directions.

We remark that in both bases global antiunitary transformations, such as $\mathcal{T} = \mathcal{K}\sigma_y$, act as constant operators in \mathbf{k} space. To switch conventions, one must transform them same as other operators, $\tilde{\mathcal{T}} = W_{-\mathbf{k}} \mathcal{T} W_{\mathbf{k}}^{-1} = \mathcal{T}$, where we used that $W_{\mathbf{k}}^{-1} = W_{-\mathbf{k}} = W_{\mathbf{k}}^*$, as W is diagonal and proportional to the identity in spin space.

APPENDIX C: WEAK TOPOLOGICAL SUPERCONDUCTORS (CLASS C AND D)

Weak indices are also present in other symmetry classes [14,16,29,58], and our considerations can be extended to topological superconductors. In 3D there are analogous 2D \mathbb{Z} and $2\mathbb{Z}$ indices in classes D and C, respectively; these are Chern numbers of the Bogoliubov–de Gennes (BdG) Hamiltonians, and the same reasoning applies as in class A detailed in Sec. II.

In other cases, however, the presence of charge conjugation symmetry (\mathcal{C}) has a more important role. We briefly review class D in two dimensions as an example. In class D there are 1D \mathbb{Z}_2 indices that serve as $d-1$ -dimensional weak indices in a 2D system,

$$v_i = \frac{1}{\pi} \oint \text{Tr } \mathcal{A} \pmod{2}, \quad (\text{C1})$$

where the integration contour is along an invariant line on the edge of the BZ, parametrized as $\mathbf{G}_i/2 + t\epsilon_{ij}\mathbf{G}_j$, $t \in [0,1]$. Similarly to the weak \mathbb{Z}_2 in 3D TIs, the value v'_i on a parallel invariant line through the Γ point ($t\epsilon_{ij}\mathbf{G}_j$, $t \in [0,1]$) is not independent; it is related through the 2D strong index $C \in \mathbb{Z}$ such that $C \equiv (v_i + v'_i) \pmod{2}$. The weak vector

$$\mathbf{G}^v = \frac{1}{2} \sum_i v_i \mathbf{G}_i \quad (\text{C2})$$

also transforms as \mathbf{k} -space vectors under all space group operations. This shows that 2D crystals with rhombic and square lattices only allow $\mathbf{G}^v = (\frac{1}{2}, \frac{1}{2})$ (in primitive basis) and three- or sixfold rotational symmetry does not allow any nontrivial weak vector. This known result [29] is generalized here and applies to arbitrary nonsymmorphic space group symmetries with the same point group part.

In order to prove the transformation properties of the 1D weak \mathbb{Z}_2 indices in class D, we have to switch to the BZ periodic convention, as $\text{Tr}_{\text{occ}} \oint \mathcal{A}$ is quantized only in a periodic basis and gauge. A space group operation g in this basis is represented as $U^{ab} = U_0^{ac} \delta^{cb} e^{-i\mathbf{k}\delta\mathbf{R}_b}$, where $\delta\mathbf{R}_a$ is the lattice vector of the unit cell in which site a of the unit cell at $\mathbf{R} = 0$ ends up after the application of g . U_0 is \mathbf{k} independent and we set it to the identity without loss of generality. The set $\delta\mathbf{R}_a$ depends on the choice of the unit cell, and a basis transformation redefining the unit cell has the same form with $\delta\mathbf{R}_a$ showing the change of unit cell position to which site a is assigned. Now we are in a position to prove two things at once: The 1D \mathbb{Z}_2 indices in class D transform in a simple fashion under SG operations and are insensitive to the choice of the real-space unit cell.

We introduce the band-flattened Hamiltonian, $\mathcal{Q} = \mathbb{1} - 2\mathcal{P}$; it has the same properties as H except all particle/hole-like bands have energy ± 1 . Charge conjugation symmetry $\mathcal{C} = \tau_x \mathcal{K}$ imposes $\mathcal{Q}_{\mathbf{k}} = -\tau_x \mathcal{Q}_{-\mathbf{k}}^* \tau_x$; for \mathcal{P} it means $\mathcal{P}_{\mathbf{k}} = \mathbb{1} - \tau_x \mathcal{P}_{-\mathbf{k}}^* \tau_x$. The particle- and hole-like states are related by Hermitian conjugation. This, in general, implies $U_{\mathbf{k}} = \tau_x U_{-\mathbf{k}}^* \tau_x$; for the diagonal form we use this means every \mathbf{R}_a has to appear twice. This is a consequence of double counting degrees of freedom; the creation and annihilation operators of the same state must live on the same lattice site. We remark that our proof relies on the assumption that charge conjugation is strictly local. While this is always true for BdG Hamiltonians, it may not be valid in insulators with effective particle-hole symmetry that exchanges lattice sites [58]. We find

$$i \oint_0^{\mathbf{G}} \text{Tr}(\mathcal{P} U^\dagger dU) = -\frac{i}{2} \oint_0^{\mathbf{G}} \text{Tr}(U^\dagger dU) \quad (\text{C3})$$

$$= -\frac{1}{2} \oint_0^{\mathbf{G}} \sum_a d\mathbf{k} \delta\mathbf{R}_a = -\frac{1}{2} \sum_a \mathbf{G} \delta\mathbf{R}_a, \quad (\text{C4})$$

where \mathbf{G} is the reciprocal lattice vector along which the integration contour for $\text{Tr}_{\text{occ}} \oint \mathcal{A}$ is oriented. Because of the doubling of orbitals, the right-hand side of the equation is always an integer multiple of 2π . Comparing with (A5), we see that a change of the unit cell or a space group operation (with the appropriate transformation on \mathbf{k} space) does not change the value of $\text{Tr}_{\text{occ}} \oint \mathcal{A}$, which is only defined modulo 2π .

APPENDIX D: NO CONSTRAINTS ON STRONG TIs

In general, a topological phase from Kitaev's periodic table, protected by a global symmetry of the ten AZ classes is robust against breaking lattice symmetry, such as strong TI in 3D. If a phase is compatible with a group G , then it is also compatible with any space group that is a subgroup of G . This is simply true because the topological protection does not rely on G . All the symmetry restrictions in G can do is to rule out certain phases in the original classification. A subgroup cannot rule out more phases, as it poses less restrictions. Of course, it is possible to have phases that are protected by G (and the global symmetry); then breaking G down to a subgroup can either allow more phases or protect less. For example, as we saw, nonsymmorphic symmetry can give interesting results about

weak indices, because they rely on the translation part of the space group for protection.

As every crystallographic space group is a subgroup of either SG #229 ($Im\bar{3}m$) or #191 ($P6/mmm$), finding examples of strong TIs in both of these crystal structures proves that crystal symmetry cannot forbid strong TIs: Starting from either of these maximally symmetric examples and weakly breaking some of the lattice symmetries, one can produce a system with any SG without leaving the strong TI phase.

In our tight-binding examples we have a single site per unit cell with two orbitals, four bands in total. One of the orbitals is a spinful s orbital, transforming under rotations with the canonical $SU(2)$ representation and even under inversion. The other orbital transforms the same way under proper rotations, but odd under inversion; such orbitals naturally arise through crystal-field splitting of p orbitals in a spin-orbit coupled ion. We introduce the Pauli matrices τ to act on the space of the two orbitals; now proper rotations by angle \mathbf{n} are represented as $\exp(\frac{i}{2}\mathbf{n} \cdot \boldsymbol{\sigma})$, inversion as τ_z and time-reversal as $\mathcal{T} = \sigma_y \mathcal{K}$. Both minimal models have the same form that guarantees that

they are invariant under the full symmetry group,

$$H(\mathbf{k}) = \sum_{\boldsymbol{\delta}} \{ \sin(\mathbf{k} \cdot \boldsymbol{\delta})(\boldsymbol{\delta} \cdot \boldsymbol{\sigma})\tau_x + [m - \cos(\mathbf{k} \cdot \boldsymbol{\delta})]\tau_z \}, \quad (\text{D1})$$

where the sum runs over nearest-neighbor vectors. By tuning m we can enter the strong TI phase. This can be easily checked by counting inversion eigenvalues.

This result is expected based on the band inversion picture. The Γ point is always of maximal symmetry; it is possible to have a band inversion only at the Γ point, resulting in a strong TI with trivial weak indices. We can also rationalize this result from the effective field theory point of view. The strong TI phase is characterized by the topological θ term in the long-wavelength electromagnetic action, a theory that possesses continuous translation and rotation symmetries. While a microscopic theory with full Galilean invariance is not possible, we showed that the maximally symmetric crystal structures are all compatible with this emergent behavior.

-
- [1] M. Z. Hasan and C. L. Kane, *Rev. Mod. Phys.* **82**, 3045 (2010).
 - [2] M. Z. Hasan and J. E. Moore, *Annu. Rev. Condens. Matter Phys.* **2**, 55 (2011).
 - [3] X.-L. Qi and S.-C. Zhang, *Rev. Mod. Phys.* **83**, 1057 (2011).
 - [4] A. Altland and M. R. Zirnbauer, *Phys. Rev. B* **55**, 1142 (1997).
 - [5] A. P. Schnyder, S. Ryu, A. Furusaki, and A. W. W. Ludwig, *Phys. Rev. B* **78**, 195125 (2008).
 - [6] A. Kitaev, in *American Institute of Physics Conference Series*, American Institute of Physics Conference Series, edited by V. Lebedev and M. Feigel'Man (American Institute of Physics, College Park, MD, 2009), Vol. 1134, pp. 22–30.
 - [7] J. E. Moore and L. Balents, *Phys. Rev. B* **75**, 121306 (2007).
 - [8] R. S. K. Mong, J. H. Bardarson, and J. E. Moore, *Phys. Rev. Lett.* **108**, 076804 (2012).
 - [9] Z. Ringel, Y. E. Kraus, and A. Stern, *Phys. Rev. B* **86**, 045102 (2012).
 - [10] I. C. Fulga, B. van Heck, J. M. Edge, and A. R. Akhmerov, *Phys. Rev. B* **89**, 155424 (2014).
 - [11] Y. Yoshimura, A. Matsumoto, Y. Takane, and K.-I. Imura, *Phys. Rev. B* **88**, 045408 (2013).
 - [12] T. Morimoto and A. Furusaki, *Phys. Rev. B* **89**, 035117 (2014).
 - [13] Y. Ran, Y. Zhang, and A. Vishwanath, *Nat. Phys.* **5**, 298 (2009).
 - [14] Y. Ran, [arXiv:1006.5454](https://arxiv.org/abs/1006.5454).
 - [15] R.-J. Slager, A. Mesaros, V. Juričić, and J. Zaanen, *Phys. Rev. B* **90**, 241403 (2014).
 - [16] I. C. Fulga, D. I. Pikulin, and T. A. Loring, *Phys. Rev. Lett.* **116**, 257002 (2016).
 - [17] Y. Qi and L. Fu, *Phys. Rev. Lett.* **115**, 236801 (2015).
 - [18] D. F. Mross, A. Essin, J. Alicea, and A. Stern, *Phys. Rev. Lett.* **116**, 036803 (2016).
 - [19] F. Lu, B. Shi, and Y.-M. Lu, [arXiv:1701.00784](https://arxiv.org/abs/1701.00784).
 - [20] B. Rasche, A. Isaeva, M. Ruck, S. Borisenko, V. Zabolotnyy, B. Büchner, K. Koepernik, C. Ortix, M. Richter, and J. van den Brink, *Nat. Mater.* **12**, 422 (2013).
 - [21] K. Majhi, K. Pal, H. Lohani, A. Banerjee, P. Mishra, A. K. Yadav, R. Ganesan, B. Sekhar, U. V. Waghmare, and P. A. Kumar, [arXiv:1605.01613](https://arxiv.org/abs/1605.01613).
 - [22] G. Autès, A. Isaeva, L. Moreschini, J. C. Johannsen, A. Pisoni, R. Mori, W. Zhang, T. G. Filatova, A. N. Kuznetsov, L. Forró, W. van den Broek, Y. Kim, K. S. Kim, A. Lanzara, J. D. Denlinger, E. Rotenberg, A. Bostwick, M. Grioni, and O. V. Yazyev, *Nat. Mater.* **15**, 154 (2016).
 - [23] B. Yan, L. Müchler, and C. Felser, *Phys. Rev. Lett.* **109**, 116406 (2012).
 - [24] P. Tang, B. Yan, W. Cao, S.-C. Wu, C. Felser, and W. Duan, *Phys. Rev. B* **89**, 041409 (2014).
 - [25] G. Yang, J. Liu, L. Fu, W. Duan, and C. Liu, *Phys. Rev. B* **89**, 085312 (2014).
 - [26] C.-C. Liu, J.-J. Zhou, Y. Yao, and F. Zhang, *Phys. Rev. Lett.* **116**, 066801 (2016).
 - [27] L. Fu and C. L. Kane, *Phys. Rev. B* **76**, 045302 (2007).
 - [28] C. Fang, M. J. Gilbert, and B. A. Bernevig, *Phys. Rev. B* **86**, 115112 (2012).
 - [29] W. A. Benalcazar, J. C. Y. Teo, and T. L. Hughes, *Phys. Rev. B* **89**, 224503 (2014).
 - [30] R.-J. Slager, A. Mesaros, V. Juričić, and J. Zaanen, *Nat. Phys.* **9**, 98 (2013).
 - [31] C.-K. Chiu, H. Yao, and S. Ryu, *Phys. Rev. B* **88**, 075142 (2013).
 - [32] T. Morimoto and A. Furusaki, *Phys. Rev. B* **88**, 125129 (2013).
 - [33] Y.-M. Lu and D.-H. Lee, [arXiv:1403.5558](https://arxiv.org/abs/1403.5558).
 - [34] C. Fang and L. Fu, *Phys. Rev. B* **91**, 161105 (2015).
 - [35] K. Shiozaki and M. Sato, *Phys. Rev. B* **90**, 165114 (2014).
 - [36] K. Shiozaki, M. Sato, and K. Gomi, *Phys. Rev. B* **91**, 155120 (2015).
 - [37] K. Shiozaki, M. Sato, and K. Gomi, *Phys. Rev. B* **93**, 195413 (2016).
 - [38] R. S. K. Mong, A. M. Essin, and J. E. Moore, *Phys. Rev. B* **81**, 245209 (2010).

- [39] C.-X. Liu, R.-X. Zhang, and B. K. VanLeeuwen, *Phys. Rev. B* **90**, 085304 (2014).
- [40] Z. Wang, A. Alexandradinata, R. J. Cava, and B. A. Bernevig, *Nature (London)* **532**, 189 (2016).
- [41] D. Varjas, F. de Juan, and Y.-M. Lu, *Phys. Rev. B* **92**, 195116 (2015).
- [42] H. Watanabe and L. Fu, *Phys. Rev. B* **95**, 081107 (2017).
- [43] H. C. Po, A. Vishwanath, and H. Watanabe, [arXiv:1703.00911](https://arxiv.org/abs/1703.00911).
- [44] B. Bradlyn, L. Elcoro, J. Cano, M. Vergniory, Z. Wang, C. Felser, M. Aroyo, and B. A. Bernevig, [arXiv:1703.02050](https://arxiv.org/abs/1703.02050).
- [45] D. J. Thouless, M. Kohmoto, M. P. Nightingale, and M. den Nijs, *Phys. Rev. Lett.* **49**, 405 (1982).
- [46] N. Nagaosa, J. Sinova, S. Onoda, A. H. MacDonald, and N. P. Ong, *Rev. Mod. Phys.* **82**, 1539 (2010).
- [47] B. I. Halperin, *Jpn. J. Appl. Phys.* **26**, 1913 (1987).
- [48] S. A. Parameswaran, A. M. Turner, D. P. Arovas, and A. Vishwanath, *Nat. Phys.* **9**, 299 (2013).
- [49] Space groups with such screw axes are usually denoted by international symbols containing 2_1 , 3_1 , 4_1 , or 6_1 .
- [50] D. Varjas, Ph.D. thesis, University of California, Berkeley, 2016.
- [51] H. Watanabe, H. C. Po, A. Vishwanath, and M. P. Zaletel, *Proc. Natl. Acad. Sci. USA* **112**, 14551 (2015).
- [52] P. Streda, *J. Phys. C* **15**, L1299 (1982).
- [53] H. Wondratschek and U. Müller, in *International Tables for Crystallography*, edited by H. Wondratschek and U. Müller (Springer, Berlin, 2008), Vol. A1.
- [54] L. Fu, C. L. Kane, and E. J. Mele, *Phys. Rev. Lett.* **98**, 106803 (2007).
- [55] *A priori* the constraints depend on the arithmetic crystal class that is determined by the point group (geometric crystal class) and its action on the translations (Bravais lattice). Direct enumeration [53], [56], [57] reveals that the result, in fact, depends only on the Bravais lattice. This can be rationalized noting that a Bravais lattice contains arithmetic crystal classes that have a large enough point group to force certain relations among lattice vectors by mapping them to each other. As \mathbf{G}^v takes values on the same reciprocal Bravais lattice with half the spacing, the constraints are the same for every arithmetic crystal class in a Bravais lattice.
- [56] M. I. Aroyo, J. M. Perez-Mato, C. Capillas, E. Kroumova, S. Ivantchev, G. Madariaga, A. Kirov, and H. Wondratschek, *Z. Kristallogr.* **221**, 15 (2006).
- [57] M. I. Aroyo, D. Orobengoa, G. de la Flor, E. S. Tasci, J. M. Perez-Mato, and H. Wondratschek, *Acta Crystallogr. Sect. A* **70**, 126 (2014).
- [58] F. de Juan, A. Rüegg, and D.-H. Lee, *Phys. Rev. B* **89**, 161117 (2014).